

Watermarking Counterfactual Explanations

Hangzhi Guo, Firdaus Ahmed Choudhury, Tinghua Chen, Amulya Yadav
Penn State University
{hangz, fac5186, tuc579, amulya}@psu.edu

Abstract

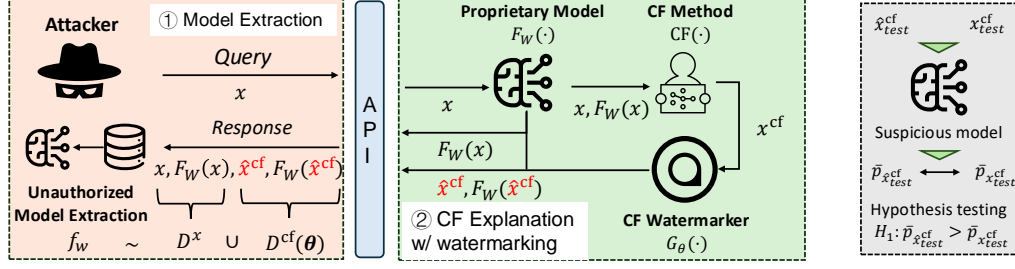
Counterfactual (CF) explanations for ML model predictions provide actionable recourse recommendations to individuals adversely impacted by predicted outcomes. However, despite being preferred by end-users, CF explanations have been shown to pose significant security risks in real-world applications; in particular, malicious adversaries can exploit CF explanations to perform query-efficient model extraction attacks on the underlying proprietary ML model. To address this security challenge, we propose *CFMark*, a novel model-agnostic watermarking framework for detecting unauthorized model extraction attacks relying on CF explanations. *CFMark* involves a novel bi-level optimization problem to embed an indistinguishable watermark into the generated CF explanation such that any future model extraction attacks using these watermarked CF explanations can be detected using a null hypothesis significance testing (NHST) scheme. At the same time, the embedded watermark does not compromise the quality of the CF explanations. We evaluate *CFMark* across diverse real-world datasets, CF explanation methods, and model extraction techniques. Our empirical results demonstrate *CFMark*'s effectiveness, achieving an F-1 score of ~ 0.89 in identifying unauthorized model extraction attacks using watermarked CF explanations. Importantly, this watermarking incurs only a negligible degradation in the quality of generated CF explanations (i.e., $\sim 1.3\%$ degradation in validity and 1.6% in proximity). Our work establishes a critical foundation for the secure deployment of CF explanations in real-world applications.

1 Introduction

Within the field of Explainable AI techniques, counterfactual (CF) explanations¹ [48, 29, 20, 13] become a popular technique for explaining the predictions generated by machine learning (ML) models [3, 35]. Given an input instance x , CF explanation methods identify a similar counterfactual instance x^{cf} that would yield a different, often more desirable, prediction from the ML model. CF explanations are useful for offering recourse to vulnerable groups. For example, when an ML model spots a student as vulnerable to dropping out of school, CF explanation techniques can suggest corrective measures to teachers, who can intervene accordingly.

Despite these usability benefits, the widespread real-world adoption of CF explanation techniques in practical ML systems remains limited. One key obstacle hindering this wider adoption is the risk of model extraction attacks through CF explanations [37]. There is an inherent tension between explainability and security: the transparency offered by CF explanations, while benefiting legitimate users, can be exploited by adversaries to extract the underlying proprietary model. As shown in Figure 1a, attackers can exploit CF explanations to execute model extraction attacks by using both the input instances and the corresponding CF explanations to train a surrogate model f_w which reproduces

¹Counterfactual explanation [48] and algorithmic recourse [44] are closely connected [46, 39]. Hence, we use both terms interchangeably throughout this paper.



(a) Illustration of ① model extraction attack using counterfactual explanations, and ② the (b) Model ownership verification procedure of generating watermarks of counterfactual explanations.

Figure 1: **Illustration of CFMark.** (a) ① Model extraction Attack. The adversaries use querying data D^x and their CF explanations $D^{cf}(\theta)$ to train a private model f_w that reproduces the predictive behavior of the proprietary model F_W . ② Watermarking. Given CF explanations x^{cf} and the proprietary model F_W , CFMark embeds a watermark into CF explanations $\hat{x}^{cf} = G_\theta(x^{cf})$. (b) Model ownership verification. If the adversaries use $D^{cf}(\theta)$ to train an extracted model f_w , our framework can *identify* this unauthorized usage via hypothesis testing.

the predictive behaviors of the proprietary model F_W . This approach is more query-efficient than traditional model extraction attacks relying only on input-output pairs [1, 49], thus posing a serious model security challenge.

Limited research has been conducted on countermeasures against model extraction attacks that exploit CF explanations. While Yang et al. [52] proposed using differential privacy in CF explanations to mitigate such attacks, their method relies on drastic perturbations to CF explanations to impede attackers, consequently reducing the explanations’ utility. Alternatively, digital watermarking presents a strong defense mechanism against model extraction attacks [17, 40, 21] by embedding identifiable markers within the model or its training data, enabling subsequent model ownership verification. However, existing digital watermarking methods do not explicitly address the vulnerabilities exposed through CF explanations, which makes existing defense mechanisms inadequate for mitigating the threat of model extractions using CF explanations.

Contributions. In this paper, we propose CFMark, a novel model-agnostic watermarking framework to safeguard against unauthorized model extraction attacks using CF explanations. CFMark involves two stages (illustrated in Figure 1): (i) *watermark embedding*: the watermark function G_θ embeds a watermark into CF explanations $\hat{x}^{cf} = G_\theta(x^{cf})$ (see Figure 1a ②). (ii) *watermark detection*: we employ a pairwise t-test to identify suspected models trained on the watermarked CF explanations (see Figure 1b). Importantly, CFMark is model-agnostic and can be used with any CF method without compromising the utility of CF explanations. Our primary contributions are in three folds:

- (Problem-Wise) We propose a novel approach to combat the model extraction attacks using CF explanations. Instead of sacrificing the quality of CF explanations for enhanced security, we propose to add watermarks to CF explanations that can provide easy identifiability of any ML model that is trained (by an adversary without authorization) using watermarked CF explanations as training data. To our knowledge, we are the first to consider watermarking CF explanations to prevent model extraction attacks.
- (Methodology-Wise) We propose a model-agnostic framework for embedding watermarks in CF explanations for model ownership verification. This framework involves a bi-level optimization to generate watermarks that can be later identified via a pairwise t-test. We further theoretically analyze the effectiveness of this verification procedure.
- (Experiment-Wise) We conduct an extensive evaluation of CFMark across various real-world datasets, CF explanation methods, and model extraction techniques. Our results show that our watermarking techniques can achieve reliable identifiability (0.89 F1-score), without trading off the utility of counterfactual explanations (only $\sim 1.3\%$ reduction in validity and $\sim 1.6\%$ in proximity).

2 Related Work

Counterfactual Explanation Techniques. Prior work on CF explanation techniques can be organized into two categories: (i) *non-parametric methods* [48, 44, 29, 45, 20, 43, 46, 19], which typically find optimal CF explanations by solving an individual optimization or searching problem, and (ii) *parametric methods* [31, 51, 28, 13, 12, 47], which adopt parametric models (e.g., a neural network model) to generate recourses. However, existing techniques fail to consider the security risks associated with providing CF explanations to end-users, which leaves the generated CF explanations vulnerable to adversaries to extract proprietary ML models.

Security and Privacy Risks in CF Explanations. Recent research has highlighted the privacy and security risks associated with model explanations [37, 36]. In particular, CF explanations can be used to carry out model extraction attacks [1, 49], linkage attacks [10], and membership inference attacks [32]. To mitigate these risks, Vo et al. [47] use feature discretization to defend against linkage attacks, but this approach lacks generalizability to defend against other attacks, such as model extraction attacks. Alternatively, differentially private CF explanations exhibit resistance to model extraction and membership inference attacks [52]. However, this approach directly deteriorates the quality of CF explanations for improved security, which limits its practicality in real-world applications.

Model Extraction Attacks and Watermarking. Our work is closely related to prior literature on model extraction (ME) attacks, which focuses on constructing private models that behave similarly to the proprietary victim model. Tramèr et al. [42] first conceptualized this attack, and later work improves the efficacy of ME attacks via active learning [5, 30], semi-supervised learning [16], adversarial examples [18, 54], and CF explanations [1, 49]. A common approach for protecting against model extraction attacks focuses on reducing the quality of ML models, such that it becomes unattractive for an adversary to conduct a model extraction attack [41]. Alternatively, digital watermarking techniques embed unique signals into either the training data [24], model parameters [38, 17], and/or model outputs [40, 21], which enables the defender (i.e., enterprise) to verify suspicious models constructed via a model extraction attack. Unfortunately, existing watermarking techniques have not explicitly considered the use of CF explanations in model extraction attacks.

3 Preliminaries

We focus on binary classification as it represents the most common setting in CF explanation research [46, 13]. Let $D_t = \{(x_i, y_i)\}_{i=1}^N$ denote a training dataset containing N data points, where $x_i \in \mathbb{R}^d$ represents the i -th input data point, and $y_i \in \{0, 1\}$ denotes its label. The enterprise service provider (i.e., defender) uses this training dataset D_t to train their proprietary predictive model $F_W : \mathcal{X} \rightarrow [0, 1]$, which outputs a probabilistic score $F_W(x)$ for a given input x .

Counterfactual Explanations. In addition to producing predictions $F_W(x)$ of input x using their predictive model, the service provider (i.e., defender) uses a CF explanation method (see Figure 1) to generate counterfactuals x^{cf} that explain the predictions of F_W on input x . Given an input x and the proprietary model F_W , a CF explanation method $\text{CF}(x; F_W)$ generates CF explanations x^{cf} which satisfies two criteria: (i) they need to be *valid* [48, 13], i.e., the CF explanations get opposite predictions from the original input $F_W(x^{\text{cf}}) = 1 - F_W(x)$, and (ii) exhibit *low proximity* [44, 13], i.e., the change from x to x^{cf} is small.

Model Extraction Attack via CF Explanations. We consider the scenario where a malicious adversary (i.e., attacker) aims to perform a model extraction attack on a proprietary machine learning model F_W . The attacker operates under the following assumptions: (i) *Black-box Access*: The attacker has black-box access to the proprietary model F_W and the CF explanation method $\text{CF}(\cdot; F_W)$, i.e., they can query the model with input x , and obtain the corresponding output probability $F_W(x)$, the corresponding CF explanations' input-output pairs $(x^{\text{cf}}, F_W(x^{\text{cf}}))$, where $x^{\text{cf}} = \text{CF}(x; F_W)$. (ii) *Attack Dataset Generation*: The attacker queries F_W with M distinct attack points, denoted as $\{(x_i)\}_{i=1}^M$, to construct a supervised attack dataset $D^x = (x_i, F_W(x_i))_{i=1}^M$. (iii) *Model Extraction*: The attacker leverages the attack dataset D^x to train an extracted ML model, $f_w : \mathcal{X} \rightarrow [0, 1]$, that closely approximates the behavior of the proprietary model, i.e., $\{f_w(x_i) \approx F_W(x_i) \mid \forall x_i \in D^x\}$.

Prior work has demonstrated that adversaries can exploit CF explanations to improve the query efficiency of model extraction attacks [1, 49]. For example, *MRCE* [1] incorporates a set of corresponding CF explanations $D^{\text{cf}} = \{(x_i^{\text{cf}}, 1 - F_W(x_i))\}_{i=1}^M$ into the attack dataset, and use both D^x

and D^{cf} for training their extracted model. *DualCF* [49] further improves the query efficiency of *MRCE* (see Appendix B for details). In this paper, we address this vulnerability by introducing a watermarking approach to protect against such attacks.

4 CFMark: A Watermarking Framework for CF Explanations

We propose CFMark, a novel watermarking framework for CF explanations to protect against model extraction attacks that use CF explanations. At a high level, CFMark consists of two stages: (i) *watermark embedding*: we design a watermarking function G_θ that can be used to embed watermarks into the CF explanations that are generated by the CF explanation method used by the defender. Specifically, G_θ inputs a CF explanation x^{cf} and outputs a watermarked CF explanation $G_\theta(x^{\text{cf}})$. These watermarked CF explanations can later be detected if malicious users use these watermarked CFs as training data for unauthorized model extraction attacks. Importantly, unlike prior methods that aggressively perturb the CF explanations, CFMark’s perturbations have little impact on the utility of CF explanations. (ii) *watermark detection*: we employ a pairwise t-test to identify any third-party black-box ML model trained on our watermarked CF explanations.

4.1 Stage 1: Watermark Embedding

In this paper, we define a θ -perturbation to the input CF explanation as our watermarking function $G_\theta(x^{\text{cf}}) = x^{\text{cf}} + \theta$, where the perturbation θ possesses the same dimension as x^{cf} (i.e., $x_i^{\text{cf}} \in \mathbb{R}^d$, and $\theta_i \in \mathbb{R}^d$). Crucially, the selection of θ involves optimizing two key objectives: (i) *detectability*: the perturbation θ should maximize the likelihood of successfully detecting an extracted ML model trained on watermarked CF explanations; (ii) *usability*: the perturbation θ should minimize the degradation of watermarked CF explanations’ quality. This degradation is quantified by the change in validity induced by the θ -perturbation watermark. Note that proximity is implicitly preserved as the perturbation θ is constrained within an l_p -norm ball (as discussed later), which inherently limits the impact on the proximity of watermarked CF explanations.

Bi-Level Optimization for Watermarking. Let $D^x = \{(x_i, F_W(x_i))\}_i^M$ denote an initial attack set, queried by adversaries from the proprietary ML model F_W using M attack points. In addition, the adversaries have access to the corresponding *watermarked* CF explanations and their predictions $D^{\text{cf}}(\theta) = \{(x_i^{\text{cf}} + \theta_i, F_W(x_i^{\text{cf}} + \theta_i)) \mid \forall (x_i, y_i) \in D^x\}$. We denote the *unwatermarked* CF explanations and their predictions as $D^{\text{cf}} = \{(x_i^{\text{cf}}, F_W(x_i^{\text{cf}})) \mid \forall (x_i, y_i) \in D^x\}$. As per our black-box access assumption, the adversary cannot access unwatermarked CF explanations. Given D^x and $D^{\text{cf}}(\theta)$, the adversaries can train an extracted model:

$$w^* = \arg \min_w \frac{1}{N} \sum_{(x_i, y_i) \in D^x \cup D^{\text{cf}}(\theta)} \mathcal{L}(f_w(x_i), y_i) \quad (1)$$

Crucially, this extracted ML model f_{w^*} is trained on the watermarked CF explanations $D^{\text{cf}}(\theta)$, which makes it possible to detect watermarks at a later stage. Intuitively, if the extracted model is trained on the watermarked explanations, this model should exhibit greater confidence in classifying watermarked explanations than unwatermarked explanations. Therefore, we formalize the *detectability* objective as the *maximization of the logarithmic difference* between model outputs from watermarked and unwatermarked CF explanations from the extracted ML models f_{w^*} (i.e., $\log(f_{w^*}(x^{\text{cf}} + \theta)) - \log(f_{w^*}(x^{\text{cf}}))$), referred as the *poison loss*. This proposed log difference loss leverages principles from information theory [2]; maximizing this loss encourages higher certainty (or less *surprises*) in classifying watermarked explanations while lowering the certainty in classifying unwatermarked counterparts.

Furthermore, to maintain the quality of CF explanations, we aim to minimize the deviation between watermarked and unwatermarked CF explanations on the original proprietary ML models F_W (i.e., $F_W(x^{\text{cf}} + \theta) \approx F_W(x^{\text{cf}})$). Hence, we formalize the *usability* objective by minimizing the Kullback-Leibler (KL) divergence between the probability outputs from the proprietary model F_W (i.e., $KL(F_W(x^{\text{cf}} + \theta) \parallel F_W(x^{\text{cf}}))$), referred as the *validity loss*. This KL-divergence term ensures similar predictions between the watermarked and unwatermarked CF explanations, thereby ensuring the quality of watermarked CF explanations.

Thus, we formulate the watermarking embedding process as this bi-level optimization problem:

$$\begin{aligned} \max_{\theta} \quad & \sum_{(x,y) \in D^{\text{cf}}} \underbrace{\log \left(\frac{f_{w^*}(x+\theta)}{f_{w^*}(x)} \right)}_{\text{Poison Loss}} - \underbrace{\text{KL} \left(F_W(x+\theta) \parallel F_W(x) \right)}_{\text{Validity Loss}}, \\ \text{s.t.} \quad & w^*(\theta) = \arg \min_w \sum_{(x,y) \in D^x} \mathcal{L}(f_w(x), y) + \sum_{(x,y) \in D^{\text{cf}}} \mathcal{L}(f_w(x+\theta), y) \end{aligned} \quad (2)$$

where λ_1 and λ_2 are hyperparameters that balance the two loss functions, Δ denotes the l_∞ -norm ball $\Delta = \{\theta_i \in \mathbb{R}^d \mid \|\theta_i\|_\infty \leq \delta\}$, and δ is a hyperparameter which denotes the maximum perturbation. The inner (min) problem solves the model extraction problem where an adversary uses attack data points D^x and the watermarked CF explanations $D^{\text{cf}}(\theta)$ as training data $D^x \cup D^{\text{cf}}(\theta)$ to extract the proprietary ML model. The outer (max) problem jointly optimizes the *detectability* and *usability* objectives for generating watermarking.

4.1.1 Improving Generalization and Mitigating Overfitting

Unfortunately, directly optimizing Eq. 2 leads to suboptimal generalization and a tendency to overfit (shown in Section 5). To address this problem, we propose to augment this formulation via two key techniques: (i) *regularization*, and (ii) *data augmentation*.

Regularization. Our preliminary experiments optimizing the bi-level formulation in Eq. 2 show a *high false positive rate* during the watermark detection stage. In particular, our detection system (discussed in Section 4.2) falsely flags benign models that are not trained using watermarked CF explanations. This is an undesirable behavior because it leads to potentially false alarms and misidentification of legitimately trained models; even if a model is trained using normal data collection procedures, it might be falsely flagged as an unauthorized extraction model.

This high false positive rate happens when the selected perturbations θ lead to high poison loss w.r.t. benign models (i.e., models not trained on watermarked CF explanations $D^{\text{cf}}(\theta)$). Essentially, the optimization of θ overfits to achieve high poison loss on any model, irrespective of whether it is trained on $D^{\text{cf}}(\theta)$ or not (as shown in Section 5). To mitigate this overfitting problem, we incorporate a regularization term to discourage the optimization of θ in achieving high poison loss exclusively for models trained on $D^{\text{cf}}(\theta)$, thereby reducing the false positive rate. Specifically, this regularization term minimizes the log difference between model outputs from watermarked and unwatermarked CF explanations from the *benign* ML models.

Data Augmentation to Improve Generalizability. As an additional measure to prevent overfitting, we enrich the training data of the extracted ML model f_w by including sampled data points from the defender’s proprietary training dataset D^t (which is feasible since the watermarking generation problem will be solved by the defender who has access to their training dataset).

4.1.2 CFMark: Our Watermarking Algorithm

Finally, we derive our new watermarking embedding:

$$\begin{aligned} \max_{\theta, \forall \theta_i \in \Delta} \quad & \frac{1}{N} \sum_{(x_i, y_i) \in D^{\text{cf}}} \underbrace{\lambda_1 \log \left(\frac{f_{w_1^*}(x_i + \theta_i)}{f_{w_1^*}(x_i)} \right)}_{\text{Poison Loss}} - \underbrace{\lambda_2 \text{KL} \left(F_W(x_i + \theta_i) \parallel F_W(x_i) \right)}_{\text{Validity Loss}} - \underbrace{\lambda_3 \log \left(\frac{f_{w_2^*}(x_i + \theta_i)}{f_{w_2^*}(x_i)} \right)}_{\text{Regularization}}, \end{aligned} \quad (3)$$

$$\text{s.t.} \quad w_1^* = \arg \min_{w_1} \sum_{(x_i, y_i) \in D^x \cup D^t \cup D^{\text{cf}}(\theta)} \mathcal{L}(f_{w_1}(x_i), y_i), \quad (4)$$

$$w_2^* = \arg \min_{w_2} \sum_{(x_i, y_i) \in D^x \cup D^t} \mathcal{L}(f_{w_2}(x_i), y_i). \quad (5)$$

where λ_3 are hyperparameters that balance the regularization strength. Compared to Eq. 2, this new formulation highlights the two proposed techniques for mitigating overfitting. First, we incorporate the *regularization term* to mitigate the overfitting to poison loss on benign models f_{w_2} , which do not use $D^{\text{cf}}(\theta)$ for training. Furthermore, we *augment the data* using sampled training data D^t for training f_{w_1} and f_{w_2} to improve the generalizability of watermarks.

The bi-level optimization problem in Eq. 3-5 is generally intractable due to its nested structure. Fortunately, we can efficiently approximate this bi-level formulation by alternating the optimization of the inner- and outer- problems using unrolling pipelines [34, 11], which has been applied to many ML problems with a bi-level formulation, e.g., meta-learning [9], poisoning attacks [15], and distributionally robust optimization [12]. Algorithm 1 details the optimization procedure for the watermarking embedding θ defined in Eq. 3-5. We iteratively solve this bi-level optimization problem via T outer steps. Each step begins by updating the weights of the extracted models w_1 and benign models w_2 . This update is performed using K unrolled gradient descent steps (Line 5-7). Next, we maximize the outer objective function (Line 8) and project θ into the feasible region Δ (Line 9). Importantly, when computing the gradient of the outer objective function w.r.t. the watermarking θ (Line 8), we look ahead several forward steps in the inner problem (Line 5-7), then backpropagate the gradient to the initial unrolling step (Line 8). This look-ahead mechanism traces the gradients back to the model unrolling stages, allowing for a more accurate approximation of θ .

Algorithm 1 Watermarking Algorithm

```

1: Hyperparameters: step size  $\alpha$ , # of watermarking steps  $T$ , # of unrolling steps  $K$ , maximum
   perturbation  $\Delta$ .
2: Input: A batch of inputs  $(x, y) \in D^x$  and their corresponding unwatermarked CF explanations
    $(x, y) \in D^{\text{cf}}$ , and sampled training data  $D^t$ .
3: Initialize: Init  $\theta$  with zeros
4: for  $i = 1 \rightarrow T$  steps do
5:   for  $k = 1 \rightarrow K$  unroll steps do
6:     Update  $w_1$  (Eq. 4),  $w_2$  (Eq. 5) using Adam
7:   end for
8:    $\theta \leftarrow \theta + \alpha \cdot \text{sign}(\nabla_{\theta} L)$   $\triangleright L := \text{Eq. 3}$ 
9:   Project  $\theta$  onto the  $l_{\infty}$ -norm ball.
10: end for
11: return  $\theta$ 

```

4.2 Stage 2: Ownership Verification

This section details the verification process for determining if a suspicious model has been trained on watermarked CF explanations. Assuming access to the predicted probability from the suspicious model, we employ a null hypothesis significance testing (NHST) scheme (Proposition 1) to identify unauthorized model extractions using watermarked CF explanations.

Proposition 1. *Suppose p_x is the posterior probability of x predicted by the suspicious model. Let x^{cf} and \hat{x}^{cf} each represent the unwatermarked and watermarked counterfactual explanations. Let $\bar{p}_{x^{\text{cf}}}$ and $\bar{p}_{\hat{x}^{\text{cf}}}$ each denote the mean of the posterior probabilities $p_{x^{\text{cf}}}$ and $p_{\hat{x}^{\text{cf}}}$ over n observations. Given the null hypothesis $H_0 : \bar{p}_{\hat{x}^{\text{cf}}} = \bar{p}_{x^{\text{cf}}} + \tau$ ($H_1 : \bar{p}_{\hat{x}^{\text{cf}}} > \bar{p}_{x^{\text{cf}}} + \tau$), where τ is a hyper-parameter, we claim that the suspicious model is trained on counterfactual explanations (with τ -certainty) if and only if H_0 is rejected.*

In practice, we randomly sample N data points from the test sets to conduct this pairwise t-test. We reject the null hypothesis H_0 if the resulting p-value is below a predetermined significance level α (we set $\alpha = 0.05$). Finally, we provide a theoretical analysis to establish the conditions for rejection of H_0 at significance level α in Theorem 4.1. The proof is provided in Appendix A.

Theorem 4.1. *We define the following quantities: $\bar{d} = \mathbf{E}(p_{\hat{x}^{\text{cf}}} - p_{x^{\text{cf}}})$ and $\tilde{d} = \sum_{i=1}^n (p_{\hat{x}_i^{\text{cf}}} - p_{x_i^{\text{cf}}})^2$. We claim that defenders owners can reject the null hypothesis $H_0 : \bar{p}_{\hat{x}^{\text{cf}}} = \bar{p}_{x^{\text{cf}}} + \tau$ (versus $H_1 : \bar{p}_{\hat{x}^{\text{cf}}} > \bar{p}_{x^{\text{cf}}} + \tau$) at significance level α , if \bar{d} and \tilde{d} satisfy that*

$$\sqrt{n^2 - n}(\bar{d} - \tau) - t_{1-\alpha} \sqrt{\tilde{d} + n\bar{d}^2} > 0 \quad (6)$$

where τ is the level of certainty and $t_{1-\alpha}$ is the $(1-\alpha)$ -quantile of t -distribution with $n - 1$ degrees of freedom and n is the sample size of x^{cf} .

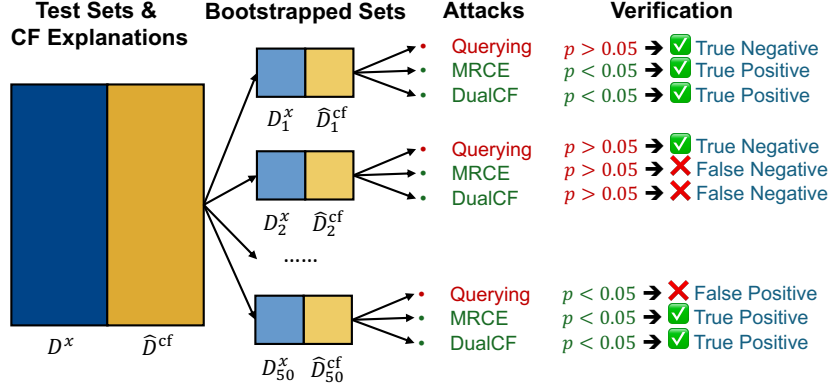


Figure 2: Illustration of the evaluation procedure for watermarking. Green indicates positive cases, and red indicates negative cases.

5 Experimental Evaluation

Datasets. We evaluate the performance of our watermarking framework using four real-world datasets: (i) *Cancer* [7] contains 569 instances and uses cell nuclei characteristics to classify tumors as malignant ($Y=1$) or benign ($Y=0$). (ii) *Credit* dataset [53] contains 30,000 instances and predicts whether a borrower will default on their payments ($Y=1$) or not ($Y=0$) based on historical payment records. (iii) *HELOC* dataset [8] collects anonymized Home Equity Line of Credit applications from real homeowners. This contains 10,459 instances, and the classifier predicts whether an applicant will repay their HELOC account within 2 years ($Y=1$) or not ($Y=0$) based on their application information. (iv) *Loan* dataset [23] contains $\sim 450k$ loan approval records across the U.S. from 1994 to 2009, and predicts whether a business defaulted on a loan ($Y=1$) or not ($Y=0$).

Attacker Models & CF Methods. We evaluate CFMark against three model extraction methods: (i) *Querying* attack [42] does not use CF explanations; instead it only uses the inputs and predictions pair D^x for training the extracted ML model. (ii) *MRCE* [1] adopts both inputs D^x and the corresponding watermarked CF explanations for training the extracted ML model. (iii) *DualCF* [49] adopts both watermarked CF explanations $D^{cf}(\theta)$ and their dual CF explanations $D^{cf}(\theta)'$ for training the extracted ML model.

We use three widely used CF methods for benchmarking: (i) *C-CHVAE* [31] is a parametric approach that generates CF explanations by perturbing the latent variables of a Variational Autoencoder (VAE) model. (ii) *DiCE* [29] is a non-parametric method that generates diverse CF explanations. (iii) *GrowingSphere* [22] is another non-parametric method that employs a random search algorithm to find valid recourses.

Evaluation Procedure & Metrics. Figure 2 illustrates the evaluation procedure of the experiment. We use a bootstrapping approach to evaluate CFMark’s ability to safeguard unauthorized model extraction attacks. Specifically, we first partition each dataset into train/test set splits. We train the proprietary model F_W from the training set, and consider the test set as a potential attack set. Next, we create 50 bootstrap subsets from the original test set. Each of these subsets was exposed to a model extraction attack. As a result, there are 50 extracted models for each attack method, CF explanation, and dataset combination. Extracted models trained on watermarked CF explanations (e.g., MRCE, DualCF) are considered positive, while those trained without (e.g., Querying Attack) are negative. Next, for each extracted model, we perform the ownership verification procedure (in Proposition 1). Specifically, our framework outputs *positive* (i.e., flags a model as being trained on watermarked CFs) if the p -value of the ownership verification is less than 0.05. Otherwise, we consider the output of our detection system as *negative*. We calculate true/false positives/negatives by comparing our ownership verification results with the ground-truth values of these attacked models. In total, we experiment with 1,800 extracted models (50 subsets \times 3 attacks \times 4 datasets \times 3 CF methods) to rigorously quantify our watermarking framework’s ability to identify unauthorized model extraction attacks.

To evaluate the effectiveness of CFMark, we report the $F-I$ score on measuring how accurate CFMark is in identifying models trained on watermarked or unwatermarked CF explanations. Furthermore,

Table 1: F1 score of CFMark in identifying model extraction attacks using watermarked CF explanations.

CF Method	Cancer	Credit	HELOC	Loan
C-CHVAE	0.90	0.52	0.87	0.90
DiCE	0.95	0.98	0.93	0.93
Growing Sphere	1.00	0.92	0.89	0.83

Table 2: Evaluation of the CF Explanations. Watermarked CF explanations (i.e., WM.) achieve comparative validity (i.e., Val.) and proximity (i.e., Prox.) as their unwatermarked counterparts (i.e., Original).

CF Method	Cancer		Credit		HELOC		Loan	
	Val.	Prox.	Val.	Prox.	Val.	Prox.	Val.	Prox.
CCHVAE	Original	1.0 3.23	1.0 4.40	1.0 3.73	1.0 6.90			
	WM.	0.99 3.27	0.98 4.42	0.94 3.43	1.0 6.92			
	Change (%)	1.01 1.23	2.02 0.45	6.19 8.38	0 0.29			
DiCE	Original	0.99 4.21	.90 3.98	0.90 8.39	0.67 9.01			
	WM.	0.99 4.34	.90 4.05	0.89 8.43	0.67 9.03			
	Change (%)	0 3.04	0 1.74	1.12 0.48	0 0.22			
Growing Sphere	Original	1.0 3.50	0.99 5.18	1.0 3.67	1.0 7.57			
	WM.	0.98 3.52	0.98 5.21	0.98 3.73	1.0 7.62			
	Change (%)	2.02 0.57	1.02 0.58	2.02 1.62	0 0.66			

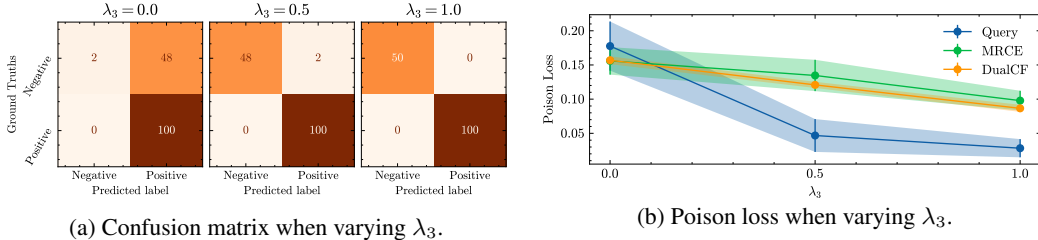


Figure 3: The impact of the *regularization* term on the credit dataset when using DiCE.

we use two widely used metrics to evaluate the quality of CF explanations [48, 29, 13]: (i) *Validity*, which measures the fraction of valid CF explanations x^{cf} with respect to F_W ; (ii) *Proximity*, which computes the l_1 distance between the input x and its CF explanation x^{cf} .

5.1 Evaluation Results

Watermarking Performance. Table 1 shows the effectiveness of CFMark in identifying model extraction attacks using CF explanations. In particular, across different datasets and CF methods, CFMark can accurately identify true positives and true negatives, achieving an average F1-score of 0.95, 0.91, and 0.80, across DiCE, Growing Sphere, and C-CHVAE, respectively. This result underscores CFMark’s performance in identifying unauthorized usage of CF explanations in model extraction attacks, while not misjudging models that do not use CF explanations for training models.

Validity & Proximity. Table 2 compares the validity and proximity of original (i.e., unwatermarked) x^{cf} and watermarked CF explanations \hat{x}^{cf} . It shows that watermarking CF explanations only leads to a minor degradation in quality. Specifically, compared with their unwatermarked counterparts, watermarked CF explanations exhibit an average 1.3% decrease in validity and a 1.6% increase in proximity across all datasets. This negligible degradation suggests that watermarking CF explanations provides a robust defense mechanism while preserving the utility of the explanations.

5.2 Further Analysis

Due to space constraints, our ablation analysis focuses on evaluating the Credit dataset when using DiCE. Further ablation studies are included in the Appendix.

Table 3: Ablations of the loss functions of CFMark on *credit* dataset when using DiCE. Val. (%) and Prox. (%) measure the validity decreases and proximity increases from unwatermarked to watermark CF explanations, respectively. High F1, low Val. (%), and low Prox. (%) are desirable.

Poison Loss	Validity Loss								
	Log Diff			KL			Residual		
	F1	Val. (%)	Prox. (%)	F1	Val. (%)	Prox. (%)	F1	Val. (%)	Prox. (%)
Log Diff	0	0.02	1.24	0.97	-0.30	1.76	0	-0.23	1.42
KL	0	4.49	-0.20	0.00	1.44	0.69	0	5.09	-0.18
Residual	0	0.32	0.69	1.0	-0.31	1.90	0	0.07	1.32

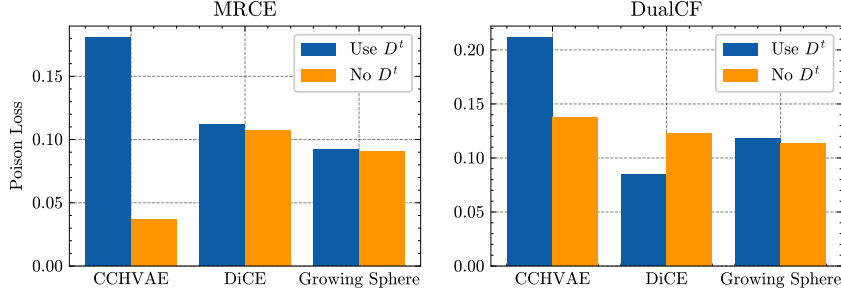


Figure 4: The impact of using training data D^t in CFMark when evaluated on credit dataset.

The Impact of Regularization. Figure 3 illustrates the importance of the *regularization* term in Eq. 3 by varying the trade-off parameter λ_3 . As shown in Figure 3a, excluding the regularization term (i.e., $\lambda_3 = 0$) results in a high false positive rate of 96% (48/50), which suggests that Query attacks are falsely identifying as positive cases. This high false positive issue is due to overfitting of the poison loss when $\lambda_3 = 0$, where the poison loss for Query attacks is as high as that for MRCE and DualCF (Figure 3b). This result highlights the overfitting challenges when optimizing the watermark θ without regularization.

On the other hand, increasing the value of λ_3 in Figure 3 leads to a significant decrease in the false positive rate and poison loss of Query attacks. In particular, the false positive rate is drastically dropped to 4% (2/50) when $\lambda_3 = 0.5$, and is further dropped to 0 when $\lambda_3 = 1.0$ (Figure 3a). This highlights the effectiveness of regularization in mitigating overfitting. Notably, this regularization term has minimal impact on the detectability of watermarked CF explanations, as evidenced by the consistent perfect true positive rate even with increasing λ_3 values.

The Impact of Data Augmentation. Figure 4 shows the impact of data augmentation (i.e., using sampled training data D_t to train the extracted model) on poison loss against the MRCE attack. This figure shows that using data augmentation helps achieve significantly better performance against the C-CHVAE explanation method, while it does not make a significant difference against DiCE and Growing Sphere.

Ablations of Loss Functions. We analyze three loss function ablations to highlight the design choice of loss functions in Eq. 3. In particular, both the poison and validity loss can adopt alternate functional forms. We experiment with three functional forms for each objective: (i) the logarithmic difference (i.e., $\log(f_{w^*}(x + \theta)) - \log(f_{w^*}(x))$), used for poison loss and the regularization term; (ii) the KL Divergence (i.e., $\text{KL}(f_{w^*}(x + \theta) \parallel f_{w^*}(x))$), used for the validity term; and (iii) the residual difference (i.e., $f_{w^*}(x + \theta) - f_{w^*}(x)$), another reasonable loss function in our setting. Table 3 reports the F1-score and the usability degradation (as measured by validity decreases (in %), and proximity increases (in %)) on different loss functions. The actual loss function combination used in the paper is represented in Gray. Importantly, compared with other ablations, our choice of loss functions achieves a high F1 score (i.e., 0.97) while maintaining minimal degradation in validity and proximity (i.e., less than 2%). Furthermore, while using residual for poisoning and KL divergence for validity loss slightly improves F1 scores, it also leads to slightly increased proximity.

Robustness to Backdoor Defense. We further study the robustness of CFMark against potential attacks by adversaries to remove these watermarks to avoid future detectability. Prior research has demonstrated that fine-tuning [26, 25] and model pruning [50, 25] are two common watermark

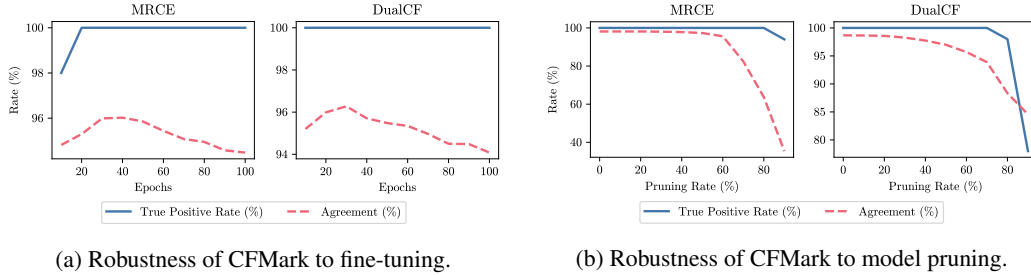


Figure 5: Robustness of CFMark to backdoor removal.

removal techniques. Therefore, we evaluate the resilience of CFMark’s watermarks against these two methods, as demonstrated in Figure 5. We use two key metrics: *true positive rate*, which measures the effectiveness of watermark detection after applying the watermark removal technique, and *agreement*, which measures the percentage of times the extracted model f_w and proprietary model F_W are in agreement (i.e., they output the same labels). This *agreement* metric reflects the effectiveness of the model extraction attack.

Figure 5a shows that CFMark watermarks are robust to model fine-tuning. The near-perfect true positive rate for both MRCE and DualCF attacks indicates strong resistance to this removal technique, even with increasing epochs of fine-tuning. Similarly, Figure 5b highlights CFMark’s robustness to model pruning when increasing the pruning rate. This figure shows that CFMark achieves a consistently high true positive rate (over 75%) for MRCE and DualCF attack detection even under reasonably high pruning rates ($\sim 60\%$). Further, we observe that increasing the pruning rate to 60% deteriorates the agreement metric; however, we argue that attackers would typically avoid high pruning rates due to the resulting utility loss in the extracted model. This result further underscores the robustness of CFMark to backdoor removal techniques.

6 Discussion & Conclusion

In this paper, we propose CFMark, the *first* watermarking framework for counterfactual explanations to identify unauthorized model extraction attacks. We formulate this watermarking framework as a bi-level optimization problem, which embeds an indistinguishable watermark into the CF explanations. These watermarks can be subsequently detected using a pairwise t-test to identify unauthorized usage of CF explanations in extracting proprietary models. Furthermore, we establish a theoretical foundation for the effectiveness of our verification procedure. Empirical results show that CFMark can achieve robust identifiability, without compromising the quality of CF explanations.

References

- [1] Aïvodji, U., Bolot, A., and Gambs, S. (2020). Model extraction from counterfactual explanations. *arXiv preprint arXiv:2009.01884*.
- [2] Ash, R. B. (2012). *Information theory*. Courier Corporation.
- [3] Bhatt, U., Xiang, A., Sharma, S., Weller, A., Taly, A., Jia, Y., Ghosh, J., Puri, R., Moura, J. M., and Eckersley, P. (2020). Explainable machine learning in deployment. In *Proceedings of the 2020 conference on fairness, accountability, and transparency*, pages 648–657.
- [4] Bradbury, J., Frostig, R., Hawkins, P., Johnson, M. J., Leary, C., Maclaurin, D., Necula, G., Paszke, A., VanderPlas, J., Wanderman-Milne, S., and Zhang, Q. (2018). JAX: composable transformations of Python+NumPy programs.
- [5] Chandrasekaran, V., Chaudhuri, K., Giacomelli, I., Jha, S., and Yan, S. (2020). Exploring connections between active learning and model extraction. In *29th USENIX Security Symposium (USENIX Security 20)*, pages 1309–1326.
- [6] Deng, L. (2012). The mnist database of handwritten digit images for machine learning research. *IEEE Signal Processing Magazine*, 29(6):141–142.

- [7] Dua, D. and Graff, C. (2017). UCI machine learning repository.
- [8] FICO (2018). Explainable machine learning challenge. <https://community.fico.com/s/explainable-machine-learning-challenge>.
- [9] Finn, C., Abbeel, P., and Levine, S. (2017). Model-agnostic meta-learning for fast adaptation of deep networks. In *International conference on machine learning*, pages 1126–1135. PMLR.
- [10] Goethals, S., Sörensen, K., and Martens, D. (2023). The privacy issue of counterfactual explanations: explanation linkage attacks. *ACM Transactions on Intelligent Systems and Technology*, 14(5):1–24.
- [11] Gu, A., Lu, S., Ram, P., and Weng, L. (2022). Min-max bilevel multi-objective optimization with applications in machine learning. *arXiv preprint arXiv:2203.01924*.
- [12] Guo, H., Jia, F., Chen, J., Squicciarini, A., and Yadav, A. (2023a). Rocoursenet: Robust training of a prediction aware recourse model. In *Proceedings of the 32nd ACM International Conference on Information and Knowledge Management, CIKM '23*, page 619–628, New York, NY, USA. Association for Computing Machinery.
- [13] Guo, H., Nguyen, T. H., and Yadav, A. (2023b). Counternet: End-to-end training of prediction aware counterfactual explanations. In *Proceedings of the 29th ACM SIGKDD Conference on Knowledge Discovery and Data Mining, KDD '23*, page 577–589, New York, NY, USA. Association for Computing Machinery.
- [14] Guo, H., Xiong, X., Zhang, W., and Yadav, A. (2023c). Relax: An efficient and scalable recourse explanation benchmarking library using jax. In *XAI in Action: Past, Present, and Future Applications*.
- [15] Huang, W. R., Geiping, J., Fowl, L., Taylor, G., and Goldstein, T. (2020). Metapoison: Practical general-purpose clean-label data poisoning. *Advances in Neural Information Processing Systems*, 33:12080–12091.
- [16] Jagielski, M., Carlini, N., Berthelot, D., Kurakin, A., and Papernot, N. (2020). High accuracy and high fidelity extraction of neural networks. In *29th USENIX security symposium (USENIX Security 20)*, pages 1345–1362.
- [17] Jia, H., Choquette-Choo, C. A., Chandrasekaran, V., and Papernot, N. (2021). Entangled watermarks as a defense against model extraction. In *30th USENIX security symposium (USENIX Security 21)*, pages 1937–1954.
- [18] Juuti, M., Szyller, S., Marchal, S., and Asokan, N. (2019). Prada: protecting against dnn model stealing attacks. In *2019 IEEE European Symposium on Security and Privacy (EuroS&P)*, pages 512–527. IEEE.
- [19] Karimi, A.-H., Barthe, G., Schölkopf, B., and Valera, I. (2020). A survey of algorithmic recourse: definitions, formulations, solutions, and prospects. *arXiv preprint arXiv:2010.04050*.
- [20] Karimi, A.-H., Schölkopf, B., and Valera, I. (2021). Algorithmic recourse: from counterfactual explanations to interventions. In *Proceedings of the 2021 ACM Conference on Fairness, Accountability, and Transparency*, pages 353–362.
- [21] Kirchenbauer, J., Geiping, J., Wen, Y., Katz, J., Miers, I., and Goldstein, T. (2023). A watermark for large language models. In *International Conference on Machine Learning*, pages 17061–17084. PMLR.
- [22] Laugel, T., Lesot, M.-J., Marsala, C., Renard, X., and Detyniecki, M. (2017). Inverse classification for comparison-based interpretability in machine learning. *arXiv preprint arXiv:1712.08443*.
- [23] Li, M., Mickel, A., and Taylor, S. (2018). “should this loan be approved or denied?”: A large dataset with class assignment guidelines. *Journal of Statistics Education*, 26(1):55–66.
- [24] Li, Y., Bai, Y., Jiang, Y., Yang, Y., Xia, S.-T., and Li, B. (2022). Untargeted backdoor watermark: Towards harmless and stealthy dataset copyright protection. *Advances in Neural Information Processing Systems*, 35:13238–13250.

- [25] Liu, K., Dolan-Gavitt, B., and Garg, S. (2018). Fine-pruning: Defending against backdooring attacks on deep neural networks. In *International symposium on research in attacks, intrusions, and defenses*, pages 273–294. Springer.
- [26] Liu, Y., Xie, Y., and Srivastava, A. (2017). Neural trojans. In *2017 IEEE International Conference on Computer Design (ICCD)*, pages 45–48. IEEE.
- [27] Madry, A., Makelov, A., Schmidt, L., Tsipras, D., and Vladu, A. (2018). Towards deep learning models resistant to adversarial attacks. In *International Conference on Learning Representations*.
- [28] Mahajan, D., Tan, C., and Sharma, A. (2019). Preserving causal constraints in counterfactual explanations for machine learning classifiers. *arXiv preprint arXiv:1912.03277*.
- [29] Mothilal, R. K., Sharma, A., and Tan, C. (2020). Explaining machine learning classifiers through diverse counterfactual explanations. In *Proceedings of the 2020 Conference on Fairness, Accountability, and Transparency*, pages 607–617.
- [30] Pal, S., Gupta, Y., Shukla, A., Kanade, A., Shevade, S., and Ganapathy, V. (2020). Activethief: Model extraction using active learning and unannotated public data. In *Proceedings of the AAAI Conference on Artificial Intelligence*, volume 34, pages 865–872.
- [31] Pawelczyk, M., Broelemann, K., and Kasneci, G. (2020). Learning model-agnostic counterfactual explanations for tabular data. In *Proceedings of The Web Conference 2020*, pages 3126–3132.
- [32] Pawelczyk, M., Lakkaraju, H., and Neel, S. (2023). On the privacy risks of algorithmic recourse. In *International Conference on Artificial Intelligence and Statistics*, pages 9680–9696. PMLR.
- [33] Pedregosa, F., Varoquaux, G., Gramfort, A., Michel, V., Thirion, B., Grisel, O., Blondel, M., Prettenhofer, P., Weiss, R., Dubourg, V., et al. (2011). Scikit-learn: Machine learning in python. *the Journal of machine Learning research*, 12:2825–2830.
- [34] Shaban, A., Cheng, C.-A., Hatch, N., and Boots, B. (2019). Truncated back-propagation for bilevel optimization. In *The 22nd International Conference on Artificial Intelligence and Statistics*, pages 1723–1732. PMLR.
- [35] Shang, R., Feng, K. K., and Shah, C. (2022). Why am i not seeing it? understanding users’ needs for counterfactual explanations in everyday recommendations. In *Proceedings of the 2022 ACM Conference on Fairness, Accountability, and Transparency*, pages 1330–1340.
- [36] Shokri, R., Strobel, M., and Zick, Y. (2021). On the privacy risks of model explanations. In *Proceedings of the 2021 AAAI/ACM Conference on AI, Ethics, and Society*, pages 231–241.
- [37] Sokol, K. and Flach, P. (2019). Counterfactual explanations of machine learning predictions: opportunities and challenges for ai safety. In *2019 AAAI Workshop on Artificial Intelligence Safety, SafeAI 2019*. CEUR Workshop Proceedings.
- [38] Song, C., Ristenpart, T., and Shmatikov, V. (2017). Machine learning models that remember too much. In *Proceedings of the 2017 ACM SIGSAC Conference on computer and communications security*, pages 587–601.
- [39] Stepin, I., Alonso, J. M., Catala, A., and Pereira-Fariña, M. (2021). A survey of contrastive and counterfactual explanation generation methods for explainable artificial intelligence. *IEEE Access*, 9:11974–12001.
- [40] Szyller, S., Atli, B. G., Marchal, S., and Asokan, N. (2021). Dawn: Dynamic adversarial watermarking of neural networks. In *Proceedings of the 29th ACM International Conference on Multimedia*, pages 4417–4425.
- [41] Tang, M., Dai, A., DiValentin, L., Ding, A., Hass, A., Gong, N. Z., and Chen, Y. (2024). Modelguard: Information-theoretic defense against model extraction attacks. In *33rd USENIX Security Symposium (Security 2024)*.

- [42] Tramèr, F., Zhang, F., Juels, A., Reiter, M. K., and Ristenpart, T. (2016). Stealing machine learning models via prediction {APIs}. In *25th USENIX security symposium (USENIX Security 16)*, pages 601–618.
- [43] Upadhyay, S., Joshi, S., and Lakkaraju, H. (2021). Towards robust and reliable algorithmic recourse. *Advances in Neural Information Processing Systems*, 34.
- [44] Ustun, B., Spangher, A., and Liu, Y. (2019). Actionable recourse in linear classification. In *Proceedings of the Conference on Fairness, Accountability, and Transparency*, pages 10–19.
- [45] Van Looveren, A. and Klaise, J. (2019). Interpretable counterfactual explanations guided by prototypes. *arXiv preprint arXiv:1907.02584*.
- [46] Verma, S., Dickerson, J., and Hines, K. (2020). Counterfactual explanations for machine learning: A review. *arXiv preprint arXiv:2010.10596*.
- [47] Vo, V., Le, T., Nguyen, V., Zhao, H., Bonilla, E. V., Haffari, G., and Phung, D. (2023). Feature-based learning for diverse and privacy-preserving counterfactual explanations. In *Proceedings of the 29th ACM SIGKDD Conference on Knowledge Discovery and Data Mining*, pages 2211–2222.
- [48] Wachter, S., Mittelstadt, B., and Russell, C. (2017). Counterfactual explanations without opening the black box: Automated decisions and the gdpr. *Harv. JL & Tech.*, 31:841.
- [49] Wang, Y., Qian, H., and Miao, C. (2022). Dualcf: Efficient model extraction attack from counterfactual explanations. In *Proceedings of the 2022 ACM Conference on Fairness, Accountability, and Transparency*, pages 1318–1329.
- [50] Wu, D. and Wang, Y. (2021). Adversarial neuron pruning purifies backdoored deep models. *Advances in Neural Information Processing Systems*, 34:16913–16925.
- [51] Yang, F., Alva, S. S., Chen, J., and Hu, X. (2021). Model-based counterfactual synthesizer for interpretation. In *Proceedings of the 27th ACM SIGKDD Conference on Knowledge Discovery and Data Mining*, KDD ’21, page 1964–1974, New York, NY, USA. Association for Computing Machinery.
- [52] Yang, F., Feng, Q., Zhou, K., Chen, J., and Hu, X. (2022). Differentially private counterfactuals via functional mechanism. *arXiv preprint arXiv:2208.02878*.
- [53] Yeh, I.-C. and Lien, C.-h. (2009). The comparisons of data mining techniques for the predictive accuracy of probability of default of credit card clients. *Expert Systems with Applications*, 36(2):2473–2480.
- [54] Yu, H., Yang, K., Zhang, T., Tsai, Y.-Y., Ho, T.-Y., and Jin, Y. (2020). Cloudleak: Large-scale deep learning models stealing through adversarial examples. In *NDSS*, volume 38, page 102.

A Proof

Theorem A.1. Let p_x denote the posterior probability of x as predicted by the suspicious model. Let x^{cf} and \hat{x}^{cf} each represent the unwatermarked and watermarked counterfactual explanations. Let $\bar{p}_{x^{cf}}$ and $\bar{p}_{\hat{x}^{cf}}$ each denote the mean of the posterior probabilities of $p_{x^{cf}}$ and $p_{\hat{x}^{cf}}$ over n observations. Define the following quantities: $\bar{d} = \mathbf{E}(p_{\hat{x}^{cf}} - p_{x^{cf}})$ and $\tilde{d} = \sum_{i=1}^n (p_{\hat{x}_i^{cf}} - p_{x_i^{cf}})^2$. We claim that dataset owners can reject the null hypothesis $H_0 : \bar{p}_{\hat{x}^{cf}} = \bar{p}_{x^{cf}} + \tau$ (versus $H_1 : \bar{p}_{\hat{x}^{cf}} > \bar{p}_{x^{cf}} + \tau$) at significance level α , if \bar{d} and \tilde{d} satisfy that

$$\sqrt{n^2 - n(\bar{d} - \tau)} - t_{1-\alpha} \sqrt{\tilde{d} + n\bar{d}^2} > 0 \quad (7)$$

where τ is the level of certainty and $t_{1-\alpha}$ is the $(1-\alpha)$ -quantile of t -distribution with $n - 1$ degrees of freedom and n is the sample size of x^{cf} .

Proof. Since both $p_{\hat{x}^{cf}}$ and $p_{x^{cf}}$ have finite means and variances. Define the distance between them as $d = p_{\hat{x}^{cf}} - p_{x^{cf}}$, which also has a finite mean and variance. Given that the data points are independent, the Central Limit Theorem (CLT) ensures the sample mean of distance, \bar{d} , converges to a Gaussian distribution as the sample size n becomes sufficiently large. Thus, we can restate the original hypothesis as:

$$\begin{aligned} H_0 : \bar{d} - \tau &= 0 \\ H_1 : \bar{d} - \tau &> 0 \end{aligned}$$

Let $\tilde{d} = \sum_{i=1}^n d_i^2$, we can construct the t -statistic as follows:

$$T := \frac{\sqrt{n}(\bar{d} - \tau)}{\sigma_d} \sim t(n - 1) \quad (8)$$

where σ_d is the standard deviation of \bar{d} and $\bar{d} - \tau$, i.e.,

$$\sigma_d^2 = \frac{1}{n-1} \sum_{i=1}^n (d_i - \bar{d})^2 = \frac{1}{n-1} (\tilde{d} + n\bar{d}^2) \quad (9)$$

To reject the hypothesis H_0 at the significance level α , we need to ensure that

$$\frac{\sqrt{n}(\bar{d} - \tau)}{\sigma_d} > t_{1-\alpha} \quad (10)$$

where $t_{1-\alpha}$ is the $(1 - \alpha)$ -quantile of t -distribution with $(n - 1)$ degree of freedom. According to equation 9 and 10, we have:

$$\sqrt{n^2 - n(\bar{d} - \tau)} - t_{1-\alpha} \sqrt{\tilde{d} + n\bar{d}^2} > 0 \quad (11)$$

□

B Details about Model Extraction Methods via CF explanations

In this section, we describe *MRCE* [1] and *DualCF* [49], two approaches that use CF explanations to perform model extraction attacks.

MRCE. Aïvodji et al. [1] showed that adversaries can perform a query-efficient model extraction attack by making half as many queries to F_W . Instead of using an attack dataset D_x of size M , the MRCE attack proceeds by using an $M/2$ sized attack dataset $D_x^{MRCE} = \{(x_i, F_W(x_i))\}_i^{M/2}$ and uses the corresponding CF explanations and their predictions $D^{cf} = \{(x_i^{cf}, 1 - F_W(x_i))\}_i^{M/2}$ as additional training data which does not require querying the ML model (since the labels on CF explanation points x^{cf} are assumed to be opposite to that of the original points x). Thus, leveraging CF explanations and their labels allows the attacker to get an M -sized training dataset by making only $M/2$ queries to F_W . Finally, the attacker use both D_x^{MRCE} and D^{cf} for training their extracted ML model $f_{w'} : \mathcal{X} \rightarrow [0, 1]$.

DualCF. Alternatively, Wang et al. [49] improves the quality of the training dataset used by the attacker to train the extracted ML model $f_{w'}$. The DualCF attack proceeds as follows: (i) the attacker queries F_W with an initial set of attack points to get $D_x^{DCF} = \{(x_i, F_W(x_i))\}_i^{M/2}$ and corresponding CF explanations $D^{cf} = \{(x_i^{cf}, 1 - F_W(x_i))\}_i^{M/2}$. (ii) The set D^{cf} is also used to query F_W to get a dual CF dataset $D^{cf'} = \{(x_i^{cf'}, 1 - (1 - F_W(x_i))\}_i^{M/2}$ (i.e., the set of CF explanations $x^{cf'}$ for the original CF explanations x^{cf} generated by the defender’s CF module). Intuitively, if the defender uses a high-quality CF explanation module, D^{cf} and $D^{cf'}$ would represent a dataset with smaller margins, and hence enable more accurate recovery (or extraction) of underlying decision boundary of F_W . Finally, the attacker use both D^{cf} and $D^{cf'}$ for training their extracted ML model $f_{w'} : \mathcal{X} \rightarrow [0, 1]$.

Protecting against Model Extraction Attacks. As described in Section 2, a common approach for mitigating model extraction attacks (in general) is to degrade the quality of the proprietary ML model F_W to disincentivize the attacker from conducting such an attack (thereby protecting the model) [41]. In the context of MRCE [1] and DualCF [49], this approach would entail degrading the quality (as measured by widely used metrics such as validity and proximity [46]) of the generated CF explanations such that it becomes unattractive for an attacker to use CF explanations as part of the training dataset used for model extraction. However, we argue that such an approach is unsatisfactory to use in real-world applications since lowering the quality of CF explanations negatively affects our ability to provide meaningful and actionable recourse to negatively affected end-users.

Therefore, in this paper, we adopt a digital watermarking approach [24, 38] to protect against these model extraction attacks that use CF explanations. Our watermarking approach can ensure that unauthorized model extraction attacks that use watermarked CF explanations can be easily identified by the defender, while maintaining the quality of the generated CF explanations.

C Implementation Details

Here we provide implementation details of our proposed framework on three datasets listed in Section 5. We provide the code, dataset, and experiment logs in the supplemental material, or be accessed in this repository: <https://github.com/BirkhoffG/CFMark>.

Software and Hardware Specifications. All experiments are run using Python (v3.10.10) with jax (v0.4.20) [4], scikit-learn (v1.2.2) [33], and jax-relax (v0.2.7) [14] for the implementations. All our experiments were run on an Ubuntu 22.04.4 LTS virtual machine on the Google Cloud Platform with an Nvidia V100 GPU.

Feature Engineering. We use the default feature engineering pipeline provided in jax-relax [14]. Specifically, for continuous features, we scale all feature values into the $[0, 1]$ range. To handle the categorical features, we transform the categorical features into numerical representations via one-hot encoding. Note that during the watermarking procedure, we treat the categorical features as immutable features, i.e., we do not add perturbations to the categorical features.

Hyperparameters. For all three datasets and CF methods, we run $T = 50$ steps for watermarking CF explanations, and set $E = 0.05$ as the maximum perturbation. The step size $\alpha = 2.5 \times \delta / T$ (based on [27]) for solving the bi-level problem in Equation 3-5. On the attack side, the model extractors have a maximum of 128 queries for extracting models reported in Table 1. In addition, Table 4 provides a detailed overview of the hyperparameters used for each dataset and CF method.

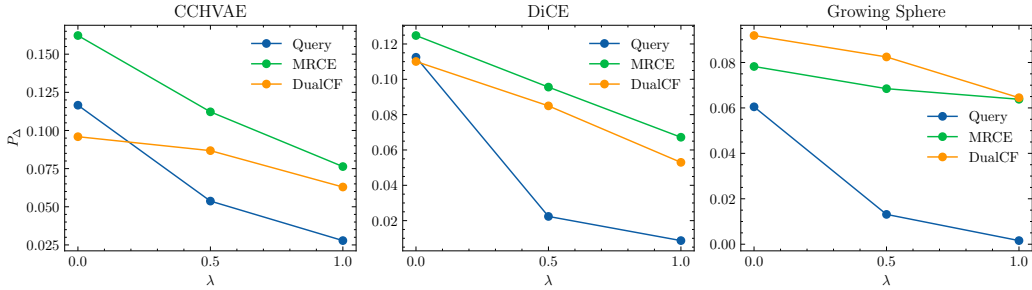
D Additional Results

Additional Ablations on Loss Functions. We provide additional ablations on loss functions of Eq. 3. Table 5 reports the F1-score and the usability degradation (as measured by validity decreases (in %), and proximity increases (in %)) on different loss functions, when evaluating the Cancer dataset using C-CHVAE. We observe similar trend as we observed in the main paper.

Confusion Matrix. Figure 8 highlights the detectability achieved by CFMark. Notably, CFMark achieves high True Positive and True Negative across all three CF methods and datasets. This result highlights the effectiveness of CFMark in watermarking CF explanations.

Table 4: Hyperparameters for each dataset.

CF Method	Dataset	Batch Size	k	learning rate	τ	Ensembels
C-CHVAE	Cancer	64	5	0.03	0.05	32
	Credit	16	10	0.01	0.05	8
	HELOC	128	5	0.1	0.05	32
	Loan	64	10	0.01	0.05	8
DiCE	Cancer	64	10	0.005	0.1	16
	Credit	64	10	0.01	0.05	8
	HELOC	64	5	0.1	0.05	8
	Loan	128	10	0.03	0.05	8
Growing Sphere	Cancer	128	10	0.02	0.05	32
	Credit	64	10	0.01	0.05	8
	HELOC	128	5	0.1	0.05	16
	Loan	128	5	0.05	0.05	16

Figure 6: The influence of the regularization term λ on the *credit* dataset.

Loss curve. Figure 9 shows the loss curve of crafting watermarks on CF explanations generated from CCHVAE, DiCE, and Growing Sphere across three datasets. The watermarking procedure is stable.

E Case Study for Watermarking CF Explanations generated from C-CHVAE on the MNIST dataset.

This section presents a case study on watermarking counterfactual (CF) explanations for image datasets. CF explanation techniques are not common choices for explaining image ML models. However, image data is valuable for understanding the impact of our watermarking technique because it allows for visual inspection and analysis of each watermarked CF explanation. This approach provides insights into how our watermarking technique influences the quality of CF explanations.

We experiment with the MNIST dataset [6] for evaluating CF explanations. We focus on image digits of either 0 or 1. We use C-CHVAE to generate CF explanations. Figure 7 showcases an example of watermarked CF explanations produced by C-CHVAE. Notably, the watermarked CF explanations maintain the visual structure observed in their unwatermarked counterparts. This observation further demonstrates that the watermarking process has little impact on the quality of CF explanations.

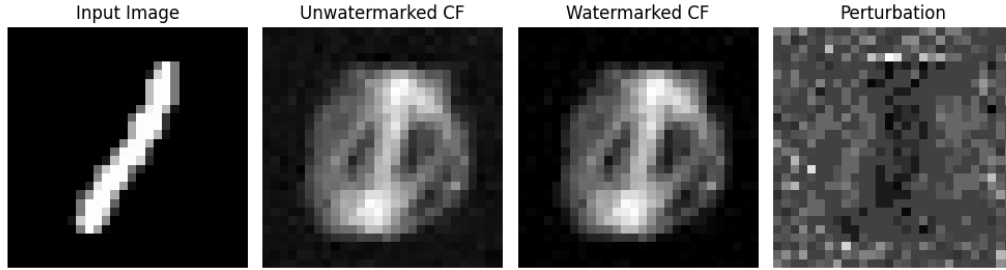
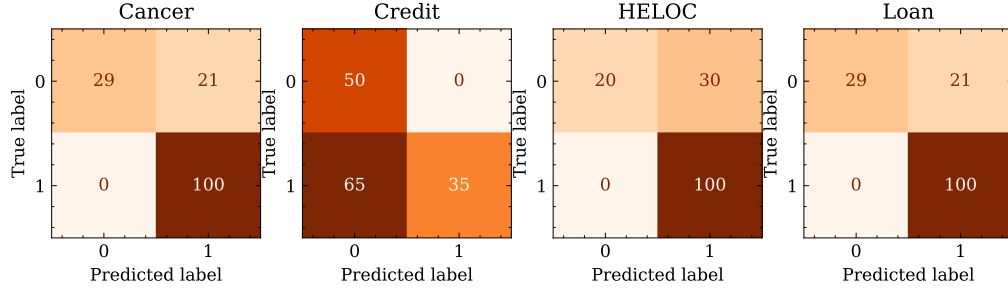


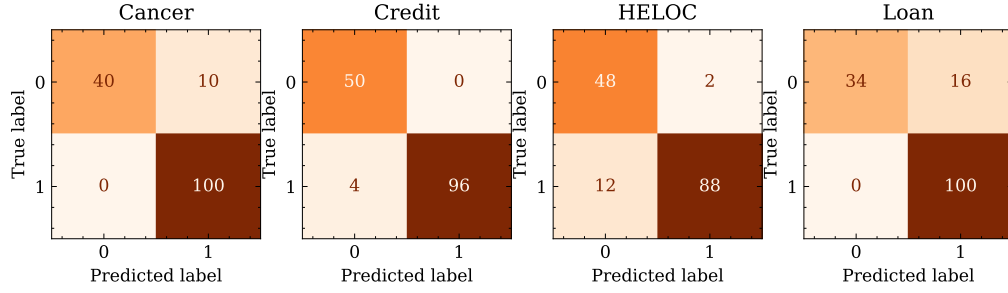
Figure 7: An example of watermarked CF explanation on MNIST.

Table 5: Ablations of the loss functions of CFMark on *cancer* dataset when using C-CHVAE.

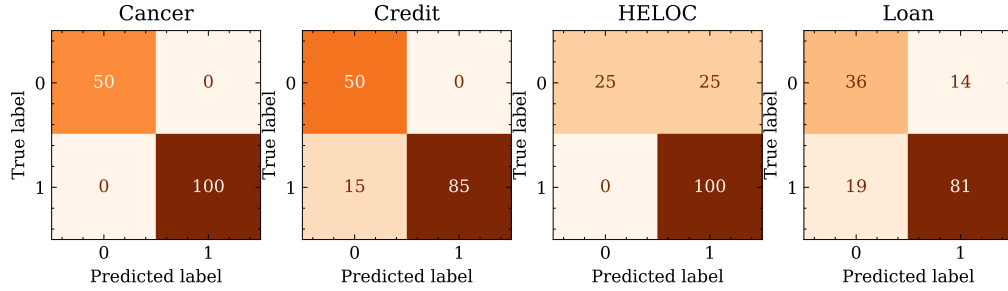
Poison Loss	Validity Loss								
	<i>Log Diff</i>			<i>KL</i>			<i>Residual</i>		
	F1	Val. (%)	Prox. (%)	F1	Val. (%)	Prox. (%)	F1	Val. (%)	Prox. (%)
<i>Log Diff</i>	0.13	9.73	0.39	0.92	2.60	0.75	0.72	8.18	0.49
<i>KL</i>	0.04	12.07	0.44	0.74	4.11	0.82	0.21	12.15	0.43
<i>Residual</i>	0.00	11.81	0.38	0.93	2.21	0.83	0.09	10.90	0.42



(a) Confusion matrix of three datasets on CCHVAE.

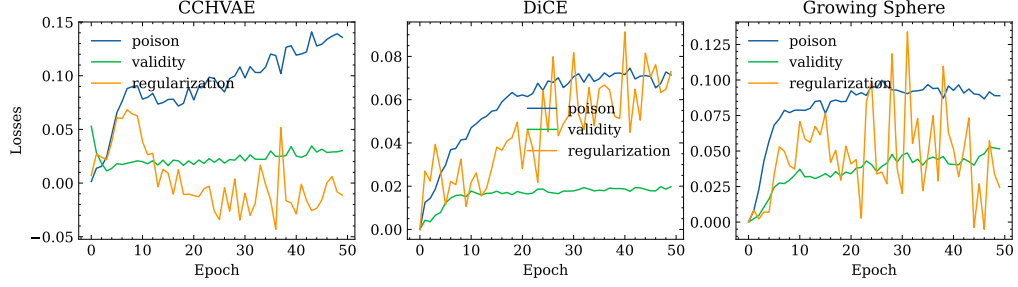


(b) Confusion matrix of three datasets on DiCE.

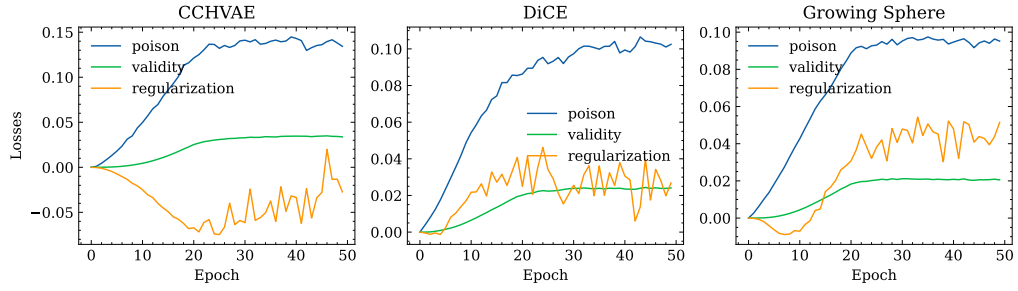


(c) Confusion matrix of three datasets on Growing Sphere.

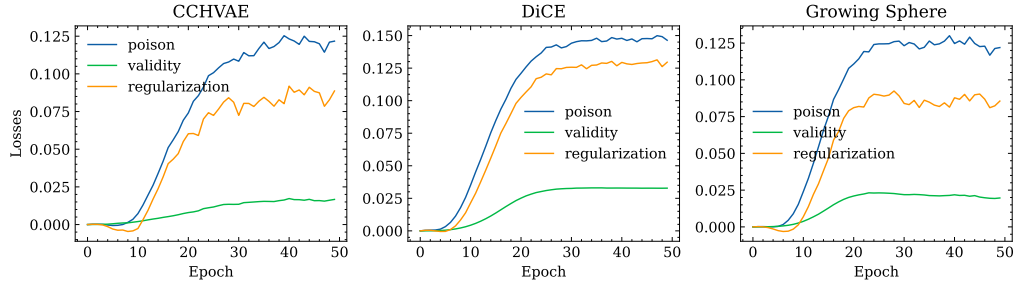
Figure 8: Confusion matrix of identifying unauthorized model extraction attacks through CF explanations from CCHVAE, DiCE, and Growing Sphere across three datasets.



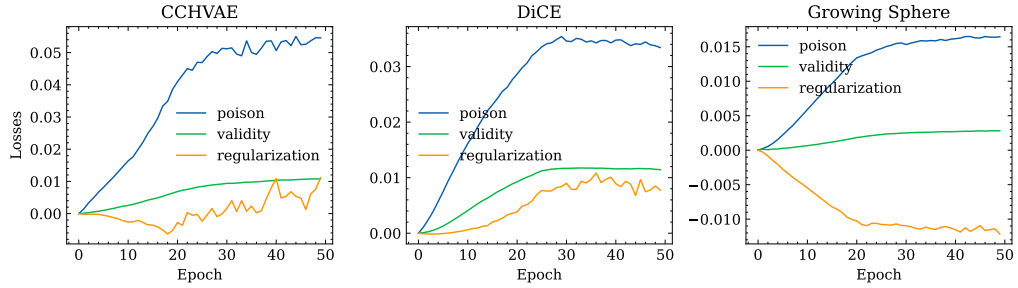
(a) Loss curves on the *Cancer* dataset.



(b) Loss curves on the *Credit* dataset.



(c) Loss curves on the *HELOC* dataset.



(d) Loss curves on the *Loan* dataset.

Figure 9: Loss curves of crafting watermarks on CF explanations generated from CCHVAE, DiCE, and Growing Sphere across three datasets.